

DIGITAL SPECTROMETERS FOR INTERPLANETARY SCIENCE MISSIONS

Robert Jarnot¹, Sharmila Padmanabhan¹, Richard Raffanti², Brian Richards², Paul Stek¹, Dan Werthimer² and Borivoje Nikolic²

April 20, 2010

Abstract

A fully digital polyphase spectrometer recently developed by the University of California Berkeley Wireless Research Center in conjunction with the Jet Propulsion Laboratory provides a low mass, power, and cost implementation of a spectrum channelizer for submillimeter spectrometers for future missions to the Inner and Outer Solar System. The digital polyphase filter bank spectrometer (PFB) offers broad bandwidth with high spectral resolution, minimal channel-to-channel overlap, and high out-of-band rejection.

INTRODUCTION

Submillimeter spectrometers have been identified as candidate instruments for future interplanetary missions to the Inner and Outer Solar System: Venus [1], Mars [2], the Jupiter system [3], and the Saturn system [4]. These missions have limited power and mass allocations for the instrument payload and are generally cost-challenged; so competitive submillimeter spectrometers need to have low mass and power, and be relatively inexpensive.

A submillimeter spectrometer comprises: an **optical system** that couples thermal emission from the scene under study and any calibration views into the instrument electronics; a **receiver front end** that down converts the incoming signal to a lower frequency band typically below 20 GHz; an **intermediate frequency signal processor**³ that amplifies the incoming signal and selects one or more sub-bands for detailed spectral analysis; and a **microwave spectrometer**⁴ that analyzes the downconverted signal with high spectral resolution. This technical note discusses an approach for significantly reducing the mass, power, and cost of the last item in this list, the microwave spectrometer, while improving capability, reliability, ease of calibration and thermal stability. This is achieved by taking advantage of digital signal processing hardware and techniques developed over the last decade for the commercial and military communications industry, and already in regular use in ground-based astronomy.

¹ Jet Propulsion Laboratory, California Institute of Technology

² UC Berkeley

³ For some systems this may be as simple as a band pass filter and an amplifier.

⁴ Spectrometer is used for both the instrument as a whole and the component that analyzes the filtered and downconverted signal. When referring to the complete instrument we will use "submillimeter spectrometer."

The bandwidth and resolution requirements for a spectrometer to provide the necessary science data for future interplanetary missions have been determined to be at least 400 MHz and 0.5 MHz respectively [5]. To efficiently meet these requirements, the University of California Berkeley Wireless Research Center (BWRC) in cooperation with the Jet Propulsion Laboratory (JPL) has developed a digital polyphase filter bank spectrometer with 750 MHz bandwidth and 4096 spectral channels. The details of the application specific integrated circuit (ASIC) developed to do the digital signal processing are presented in detail in [6] and will not be discussed here. This note will begin by describing the variety of spectrometer choices for flight missions, then discuss the polyphase spectrometer design, and finally discuss performance tests performed at JPL.

PERFORMANCE COMPARISON OF AVAILABLE SPACEBORNE SPECTROMETER TECHNOLOGIES

There has been a significant technological revolution in flight spectrometers for submillimeter instruments in the past 20 years. The most straightforward approach is to simply split the incoming signal into many narrow channels using discrete electronic filters. The JPL Microwave Limb Sounder on the Upper Research Satellite, launched in 1991, used five 15-channel **Analog Filter Banks** to accomplish the spectrum acquisition [7] with excellent results. However it is not practical to fabricate the thousands of narrow filters needed for future planetary missions.

An alternative approach is to use a dispersive structure to perform the spectral analysis. In an **Acousto-Optical Spectrometer** (AOS), the microwave signal to be analyzed is converted to an acoustic wave in a Bragg cell. The signal to be analyzed is converted into acoustic waves in a refractive medium, for example quartz. The acoustic wave modulates the index of refraction of the quartz as it passes through. A laser beam is diffracted off the lattice planes perpendicular to the acoustic wave converting the spectral information into a spatial power distribution that can then be measured with a CCD array. This approach has a successful flight heritage [8], but has high mass and power compared to alternative technologies. In addition, the AOS cannot provide the necessary bandwidth and spectral resolution from a single subsystem. A **Chirp Transform Spectrometer** (CTS) uses highly dispersive Surface Acoustic Wave delay lines and a frequency chirped local oscillator to convert frequency information into the time domain. A CTS [9] is in operation on the Microwave Instrument for the Rosetta Orbiter (MIRO) on its way to a comet rendezvous in 2014 [10]. The CTS provides the desired resolution, but with relatively high mass and power, and the bandwidth of a single implementation is limited to a percentage of the carrier frequency. Paganini [11] discusses a CTS spectrometer that achieves 400 MHz bandwidth for the SOFIA airborne observatory. Both the AOS and CTS perform a Fourier transform on the incoming data, measure the power in each FFT element, and integrate over a selected integration time. The resulting channels have a sinc^2 filter shape that has significant response in adjoining channels (see Figure 1). Also, both of these approaches require excellent thermal stability to maintain frequency calibration.

Two classes of fully digital spectrometer have been developed that are capable of providing the required bandwidth and resolution. The first of these, the **Digital Autocorrelator** (DAC) [3], has been a workhorse in radio astronomy for decades. It digitally calculates the autocorrelation function of the received signal and consists of a low resolution analog-digital converter (ADC) (typically 1 to 2 bits) followed by a shift register, multiplier, and accumulator chain. All of the electronics run at the digitizer sample rate which is the reason only a few number of bits are used. The resulting filter shapes have a sinc function. Drawbacks of the autocorrelator include loss of signal-to-noise arising from the coarse digitization (around 25% for the typical 1.5 bit ADC implementation), the need for very high speed logic

implementation, and poor performance in the presence of radio frequency interference (RFI). For a given signal bandwidth, the complexity of a digital autocorrelator scales linearly with resolution (number of channels). An additional minor drawback is that the measurement of total signal power suffers from the

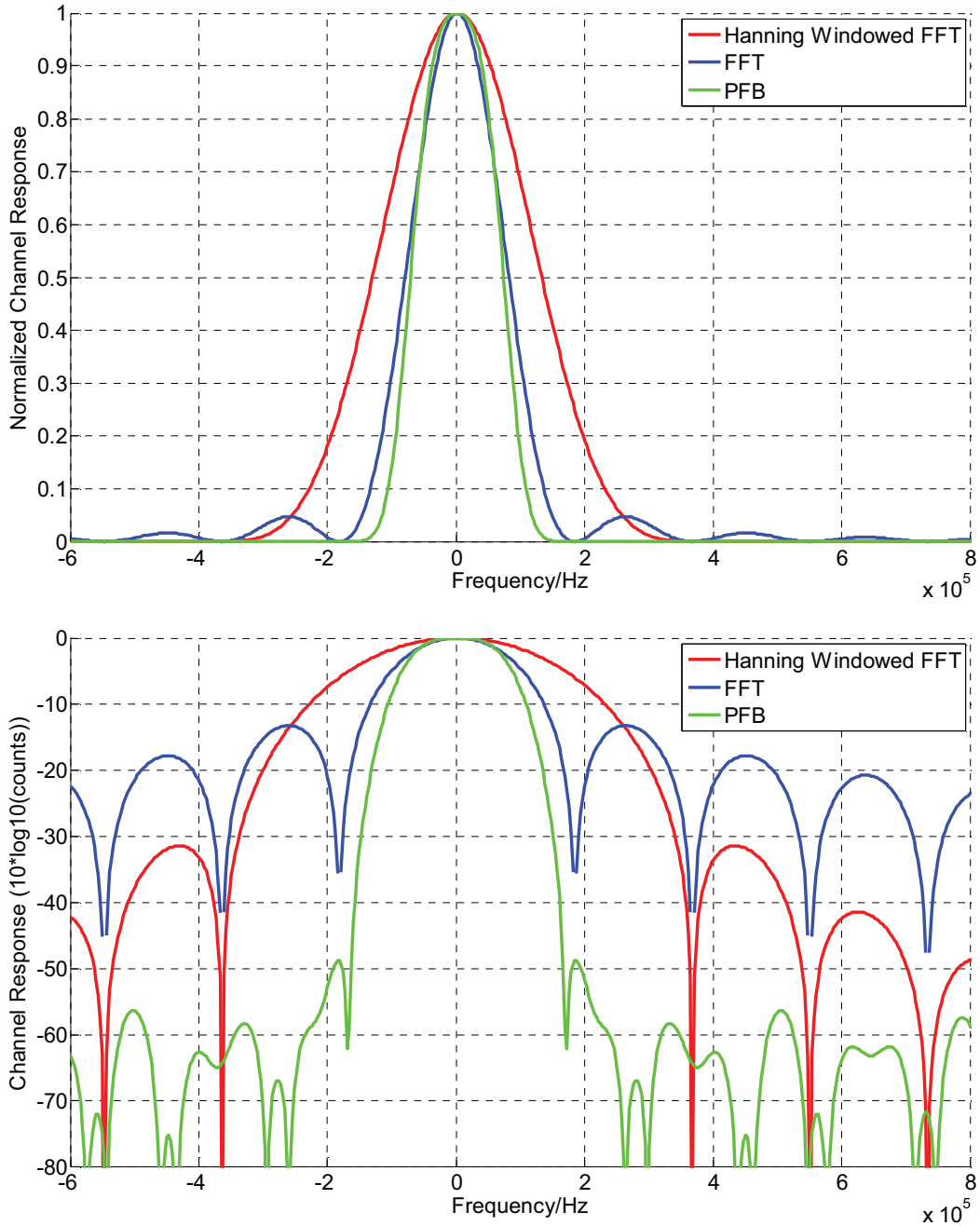


Figure 1 Theoretical channel shapes (plotted on a linear scale) of a regular FFT spectrometer compared with windowed FFT and the ASIC spectrometer using a 4-tap polyphase filter bank. (top) and the same data plotted on a log scale, illustrating the PFBs superior side lobe response.

same signal-to-noise degradation as the spectral shape measurement. This can be remedied by providing

a single analog power measurement channel, but the problem with this approach is that the bandpass shapes of the digital and analog power measurements are slightly different. This difference in passband shapes means that the high precision analog power measurement does not correspond exactly to the digital power estimate provided by the autocorrelator.

The second class of digital spectrometers samples the incoming waveform with a high speed digitizer that then feeds digital signals to a Field Programmable Gate Array (FPGA) or ASIC where the signal is decimated (spread into multiple parallel lower speed signal paths) and processed using an FFT often in combination with a windowing or filtering algorithm. The digitizer is typically 6 to 10 bits so loss of signal to noise due to finite digitization levels is minimal compared to a DAC. The two main varieties of these are **Fast Fourier Transform (FFT)** and **Polyphase Filter Bank (PFB)** spectrometers. An important advantage of this approach is that only the digitizer runs at the Nyquist frequency. The rest of the computation is parallelized and runs at a much slower rate. The filter shapes are defined through digital logic and their stability is tied to the stability of the digitizer clock. This eliminates concerns about drifting over time and temperature and can greatly simplify calibration. The FFT spectrometer is the least resource intensive approach, however this also results in a sinc^2 filter shape function. An improvement in out of band rejection can be had by apodizing the input signal using, for example, a Hanning window. This is a comparatively simple addition to the FFT but with a loss of signal to noise and a broadening of the filter response. With the polyphase filter bank described in the following sections, one can design

Table 1. Comparison of analog filter bank, AOS, CTS, Digital Autocorrelator, and the prototype ASIC PFB spectrometer. Specifications for the CTS are for a proposed new development. Existing flight CTS have demonstrated 180 MHz bandwidth with 4096 channels (0.044 MHz resolution). Lower power, wider bandwidth digital autocorrelators are currently under development. Note that the 7 W power consumption of the current PFB includes losses for the flight-like DC-DC converters, and includes the power consumption of the FPGA and interface circuitry. We have an initiative to embed the PFB into an FPGA-based C&DH [12], which potentially allows the spectrometer power consumption to be reduced to ~4.5 W by sharing DC-DC converters and eliminating the FPGA and interface circuits.

	Analog Filter bank (Aura MLS)	AOS (SWAS / ODIN)	CTS (from Paganini Thesis [11])	Digital Autocorrelator (ODIN)	PFB (ASIC prototype)
Mass	1.5 kg	7.5 kg	1.5 kg	1 kg	1.5 kg
Power	3 W	5.5 W	10 W	18 W	7 W
Spectral Bandwidth	1500 MHz	1 / 1.4 GHz	400 MHz	100 – 800 MHz (selectable)	750 MHz
Spectral Resolution	2 MHz to 96 MHz (25 chan)	1 MHz	121.2 kHz (4096 channels)	0.12 – 0.92 MHz (896 channels)	183 kHz (4096 channels)
Channel shape	Custom	sinc^2 function	sinc^2 function	sinc function (can be modified)	Custom

filter shapes to meet specific needs though with a minor increase of required computational resources as compared to the FFT approach. Figure 1 presents these 3 filter shapes.

Beyond the spectral resolution, bandwidth, and spectral response of the various spectrometer approaches, minimizing power and mass are critical to any space borne mission. Simplicity of design and minimization of part count is also paramount as this generally leads to high reliability and lower cost. Table 1 compiles the significant differences in the mass, power, spectral bandwidth and spectral resolution between existing analog and digital spectrometers designed for flight purposes. The power values include power supply losses based on a standard 28V power bus. When this was not included, we assumed 70% conversion efficiency.

DIGITAL POLYPHASE SPECTROMETER OVERVIEW

A model showing the processing functionality of a digital polyphase filter bank is shown in Figure 2. A bank of digital downconverters, each with a local oscillator (LO) at its channel center, is followed by a bank of low pass filters which define the channel shapes. Note that all of the data passes through each of the elements. There is significant duplication of computations and all of the data streams are running at the digitizer sample rate. If the channels are regularly spaced, and the channel shapes are identical, the signal flow can be rearranged into the functionally equivalent, but far less resource intensive, form shown in Figure 3. The mathematics behind this simplification can be found in references [13] and [15] or any of a number of advanced signal processing textbooks. The bank of identical low-pass filters is replaced by a single finite impulse response (FIR) filter divided into short sub taps, and the bank of LOs and mixers is replaced by an FFT.

One of the most significant advantages of the digital polyphase spectrometer arises from its

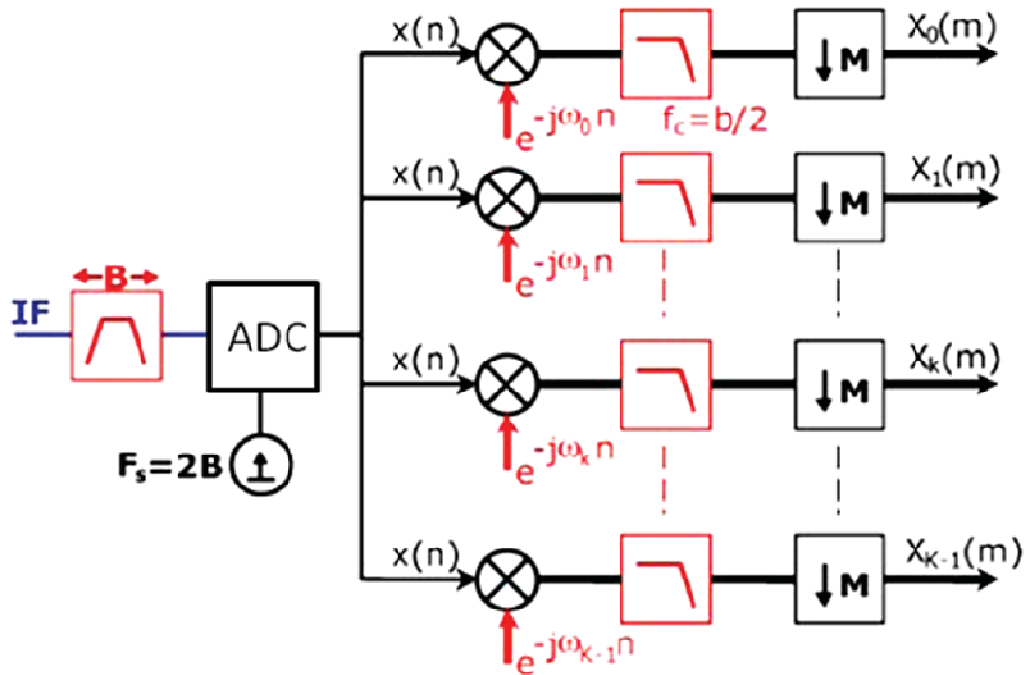


Figure 2 Schematic of the digital polyphase filter bank modeled as an array of downconverters and filters. Channel shapes are defined by a bank of low-pass filters, with channel centers set by the LO frequencies of the bank of digital mixers.[13]

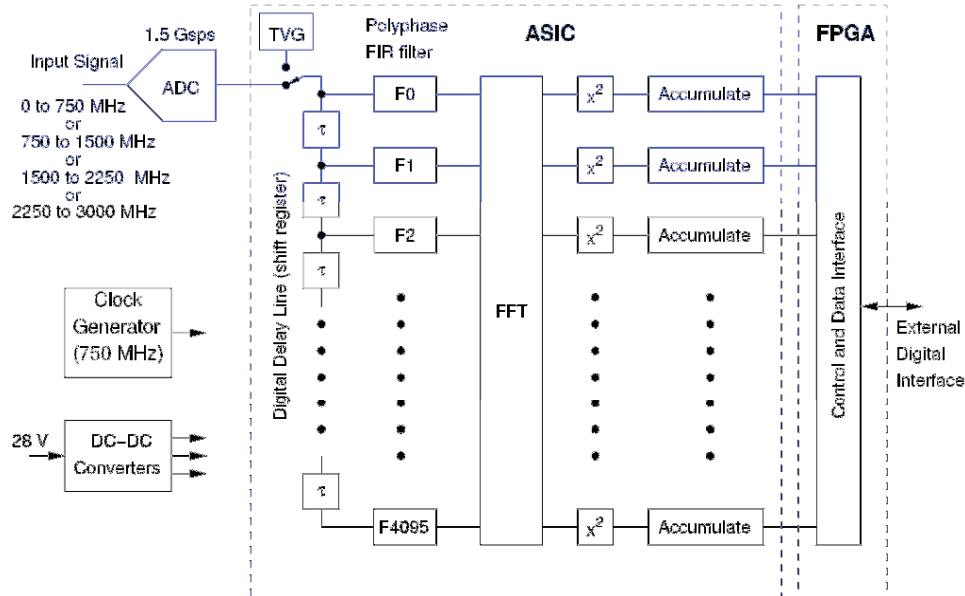


Figure 3 Simplified block diagram of a 4096 channel digital polyphase spectrometer with complex data paths. The Berkeley implementation of the ASIC uses real data paths, and hence the FFT has 8192 inputs, and the polyphase FIR filter has 8192 segments. Only half of the FFT outputs are squared and accumulated, since half of the FFT outputs in a real FFT are redundant. In the spectrometer implementation presented here, the output from the 8 bit ADC has been demultiplexed by 2 giving 16 LDVS pairs running at 750 Mbits per second running between the ADC and the ASIC. The FPGA currently serves only as a flexible interface to the instrument C&DH. It has sufficient resources to even serve as the instrument C&DH.

highly efficient scaling. When implemented in the form shown in Figure 3, increasing spectrometer resolution increases the number of filter taps preceding the FFT, but the rate at which taps are fed with data remains unaltered since it is the sample rate of the ADC. The computing overhead of the filtering operation is thus independent of the number of channels being implemented. The number of computations required to perform the FFT increases with the well known $N \log_2(N)$ relationship (where N is the number of channels). The rate that the FFT runs scales as $1/N$. So, the FFT processing overhead of the 4096-channel ASIC prototype spectrometer is only twice as large as that of a 64-channel implementation. In addition, both the filtering and FFT operations are highly amenable to hardware parallelism, allowing very efficient implementation in hardware logic.

BERKELEY PFB IMPLEMENTATION

A simplified block diagram of a radiation-hard prototype digital spectrometer is shown in Figure 3. Just three primary components are needed for the key signal, data processing and interfacing functions:

- a National Semiconductor ADC08D1520QML 1.5 GSPS, 8-bit ADC
- a custom ASIC which transforms the 1.5 GB s^{-1} data stream from the ADC into digital representation of the power spectrum of the digitized input signal, and
- a radiation-tolerant FPGA which provides a simple digital interface between the spectrometer and instrument Command and Data Handling System. The interface functions of this FPGA can be readily migrated into the C&DH FPGA, providing further simplifications at the instrument level.

The spectrometer ASIC incorporates a test vector generator (TVG), which generates a pseudo-random byte sequence in place of the ADC data, and which can be used to exercise the entire digital signal processing data flow, producing a known output spectrum. This provides a convenient way of testing the majority of the spectrometer functionality during development and qualification testing. This capability can also be invoked routinely during instrument operation to check for corruption due to single event upsets. The ADC contains several user-programmable registers to set operating mode, and parameters such as gain and offset. These registers may be subject to occasional single event induced upsets (SEU), requiring periodic refreshing of the ADC register contents. SEUs are expected to be rare in the Mars radiation environment, and our approach is to design for radiation tolerance with no permanent degradation due to SEUs, and refresh registers periodically

At the time this development effort was initiated, flight-qualifiable Xilinx Virtex 4 FPGAs were not available. These are now available with qualification suitable for a Class C instrument. All of the signal processing performed in the ASIC can be readily accomplished in a Virtex 4 SX55, however, at substantial increase in power.

Figure 4 shows the prototype digital spectrometer. The gold package at the center right of the PCB is the ADC, and the larger gold package at its 7 o'clock position is the ASIC. The black package is an Actel FPGA used to provide a simple interface to the ASIC, ADC and PLL (clock generator) registers. Also included in this prototype are DC-DC converters allowing operation from a spacecraft +28 V power bus. All components have a corresponding flight qualified version with an identical foot print. Much of the space on the board is dedicated to pads for RAM and PROM memory to allow implementation of a soft processor in the FPGA. We have recently demonstrated a C&DH with the processor implemented as

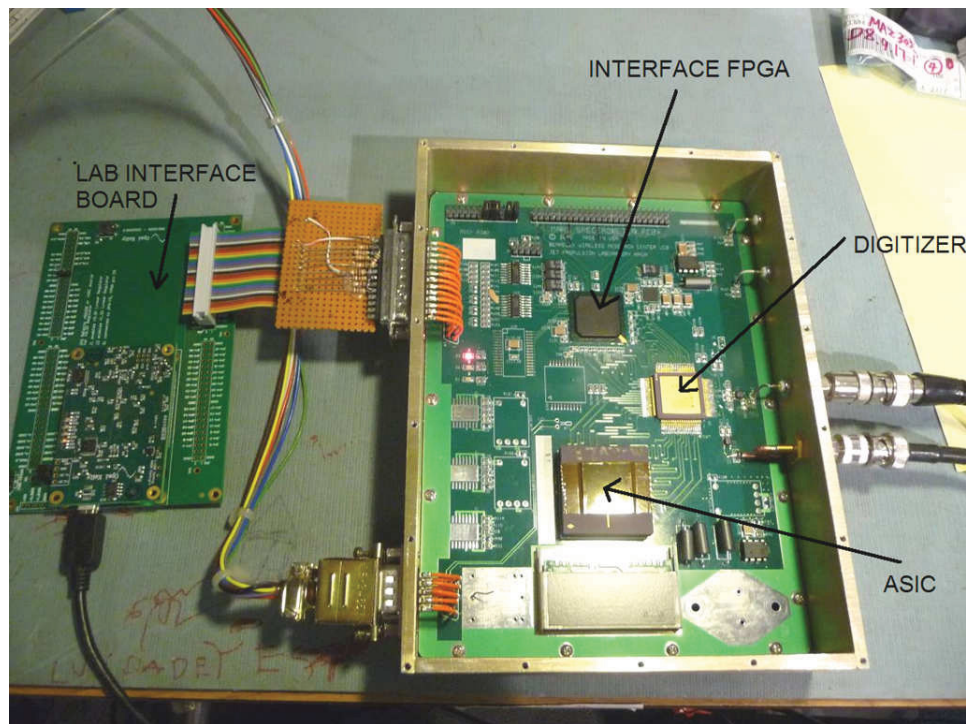


Figure 4 Photo of the rad-hard 750 MHz ASIC spectrometer chassis and board. See text for additional information.

a soft core in the same type of FPGA as the one used in the spectrometer [12]. The C&DH implements an interface to this spectrometer, allowing us to easily migrate all of the FPGA functionality in the spectrometer FPGA into the one in the C&DH, and use the C&DH DC-DC converters to power the spectrometer ICs. This will reduce the footprint of the spectrometer to about a 3” by 3” area of the spectrometer PCB instead of the 6” by 8” chassis shown in Figure 4, and will improve efficiency by reducing the number of low power DC-DC converters.

PFB PERFORMANCE TESTING

A simplified schematic of the laboratory test setup is shown in Figure 5. A pair of programmable noise sources provide ‘science like’ data, the broadband signal representing front-end receiver noise, and the narrower one simulating an atmospheric spectral signature. The two programmable

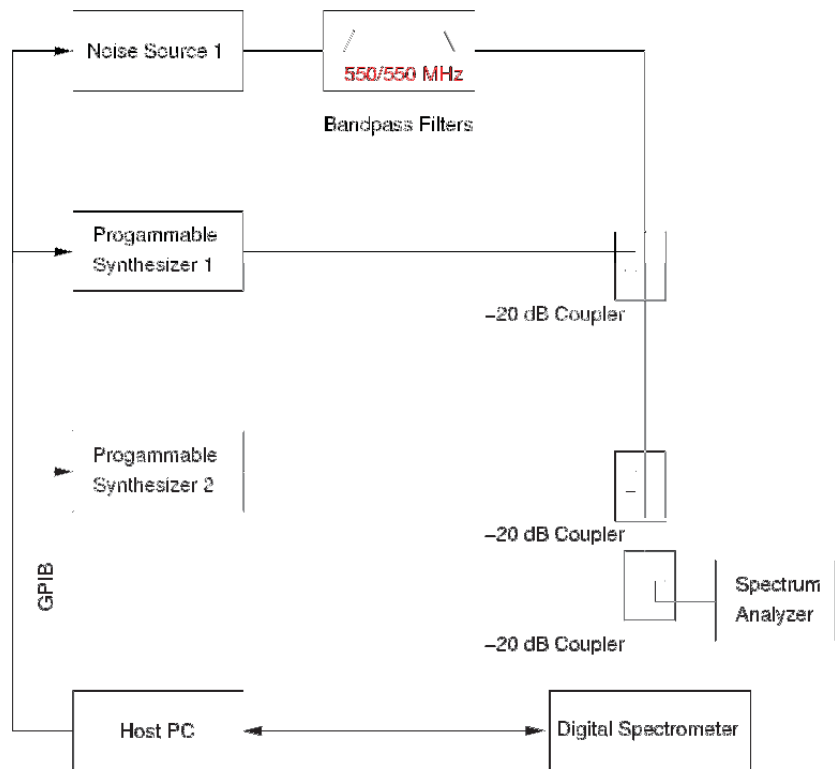


Figure 5 Simplified schematic of the laboratory test setup.

synthesizers provide tones for measuring linearity, and for observing intermodulation products. The spectrum analyzer provides an independent view of the signal being analyzed by the digital spectrometer, serving primarily to provide a quick verification of the functionality of the test setup, and serves as an aid for rapidly setting the levels of the test signals. The PC controls the test equipment and provides the control and data interface to the spectrometer. In addition to the couplers shown in the figure, additional isolation between assemblies was provided by adding pads as needed to suppress standing waves arising from minor mismatches between the various elements.

FILTER SPECTRAL SHAPE MEASUREMENTS

Spectral sweeps of individual channels of the filter bank were performed. Figure 6 shows raw measurements of successive filters. Figure 7 shows a measured channel shape (red) of the prototype polyphase spectrometer. The blue shape is the Fourier transform of the polyphase FIR filter which defines the channel shape. Note the excellent agreement between theoretical and measured shapes, with minor deviations observable in the sidelobe responses due to the finite word length (integer) arithmetic implemented in the ASIC. The polyphase filter bank is unique in its ability to produce sharp-edged channel shapes with minimal overlap without resorting to high complexity. In the particular implementation shown here, the noise bandwidth of each PFB channel is the same as the channel-to-channel spacing, implying no loss in signal-to-noise.

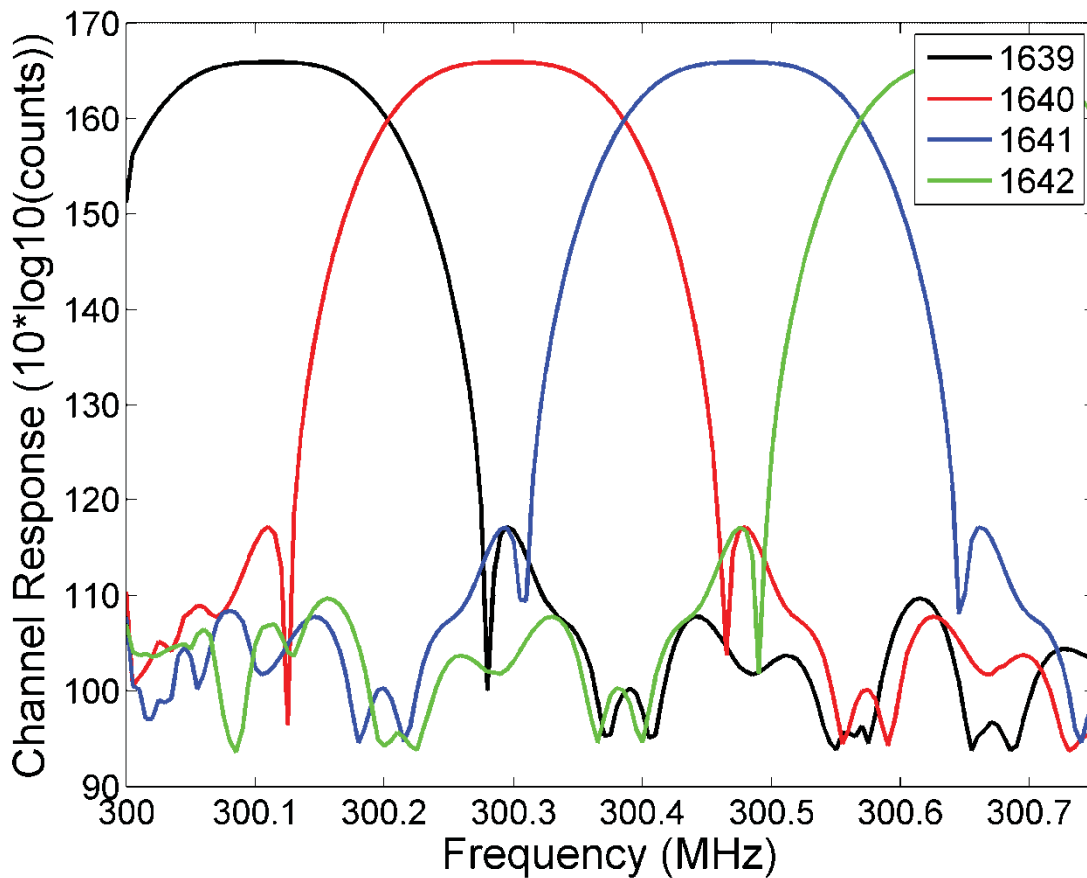


Figure 6 Measured channels shapes of the ASIC spectrometer. Note the deep and steep skirts of each digitally defined channel response, and the small amount of overlap combined with extremely low sidelobes.

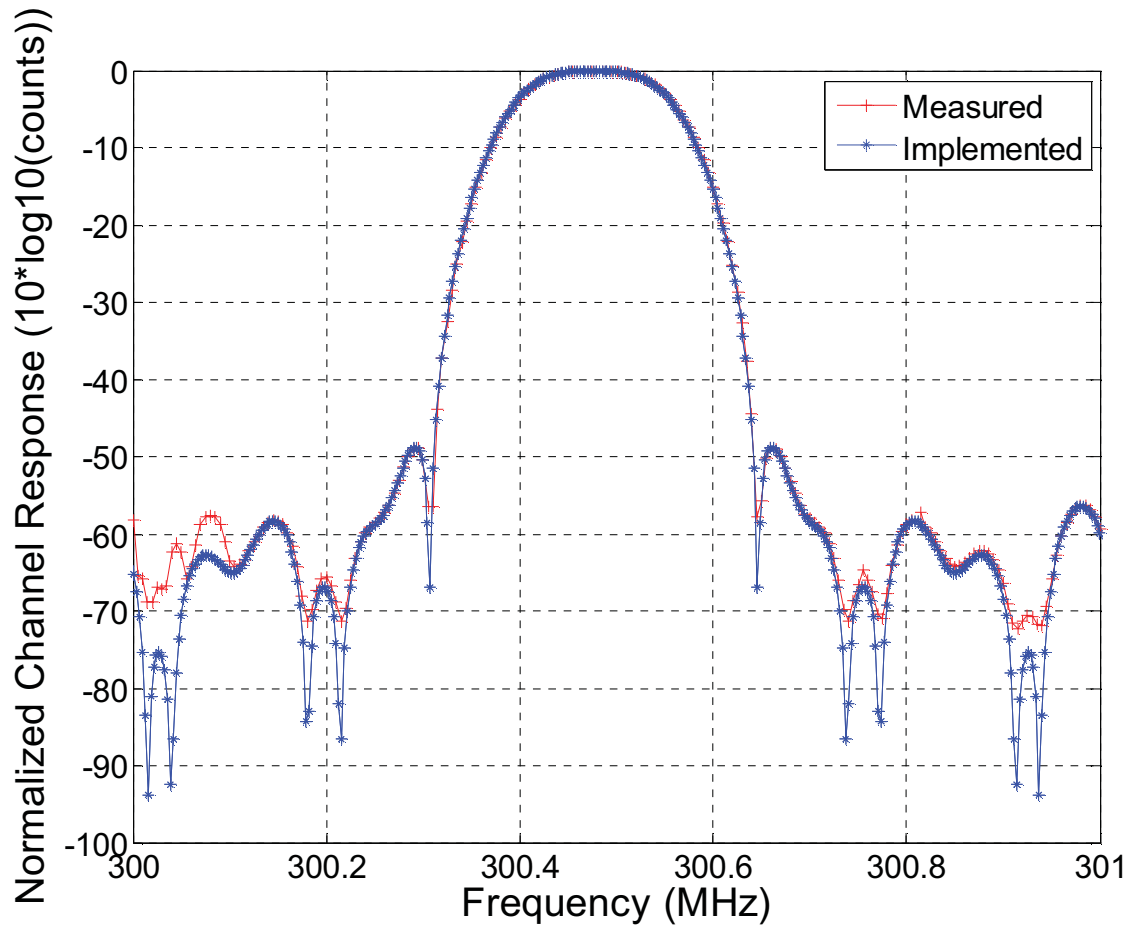


Figure 7 Comparison of implemented and measured channel shape of the 750 MHz ASIC spectrometer. See text for additional information.

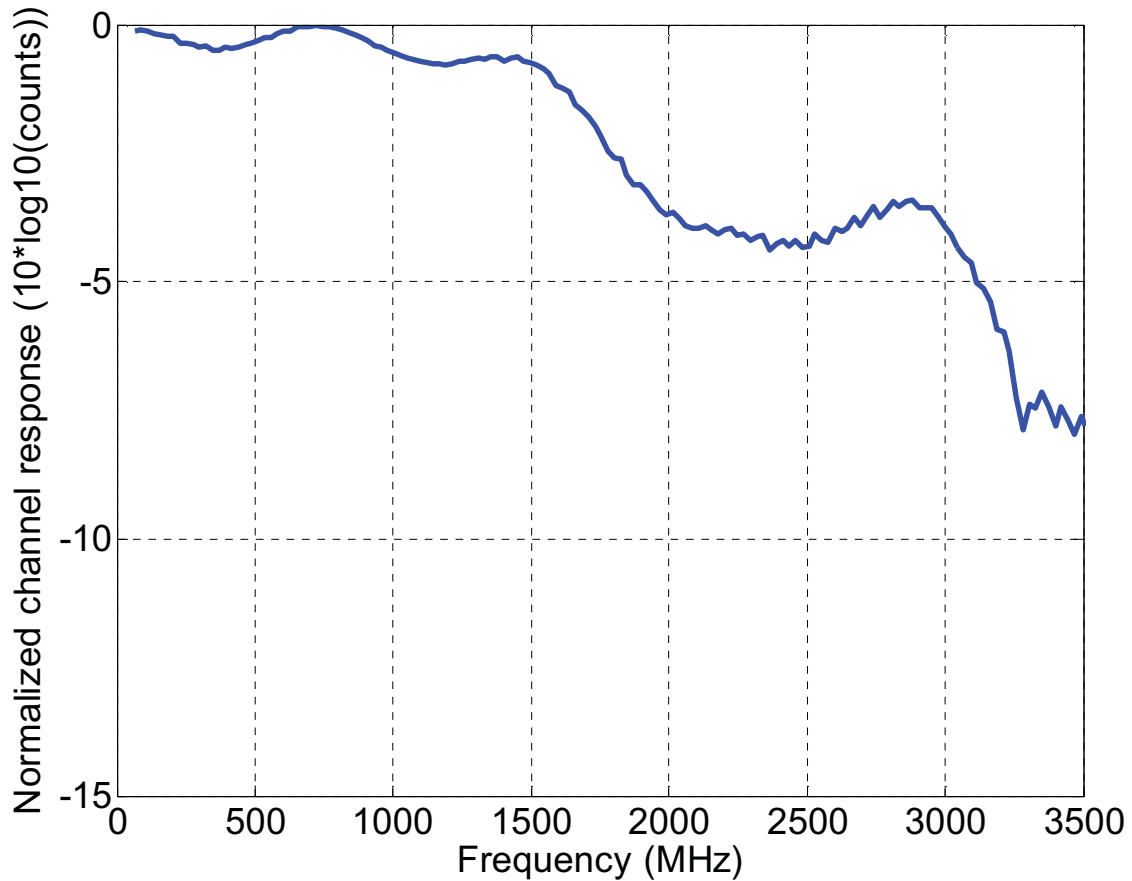


Figure 8 Sweep of the ASIC spectrometer up to 3.5 GHz, showing bandpass response through the 3rd Nyquist zone. Every 128th channel is swept in this figure.

Figure 8 shows that the ASIC spectrometer response is reasonably flat up to 3 GHz, with a more significant roll off at higher input frequencies. This means that along with use of the first Nyquist band (baseband), we can effectively use the second Nyquist (750-1500 MHz) and third Nyquist (1500-2250 MHz) bands as indicated in the block diagram in Figure 3. The ability to operate in higher Nyquist bands helps simplify the IF downconversion electronics and filtering, and provides some additional stability advantages since the ADC input stage no longer has to operate in the frequency region in which it is susceptible to the impact of 1/f noise.

STATISTICAL INTEGRATION TIME- ALLAN VARIANCE

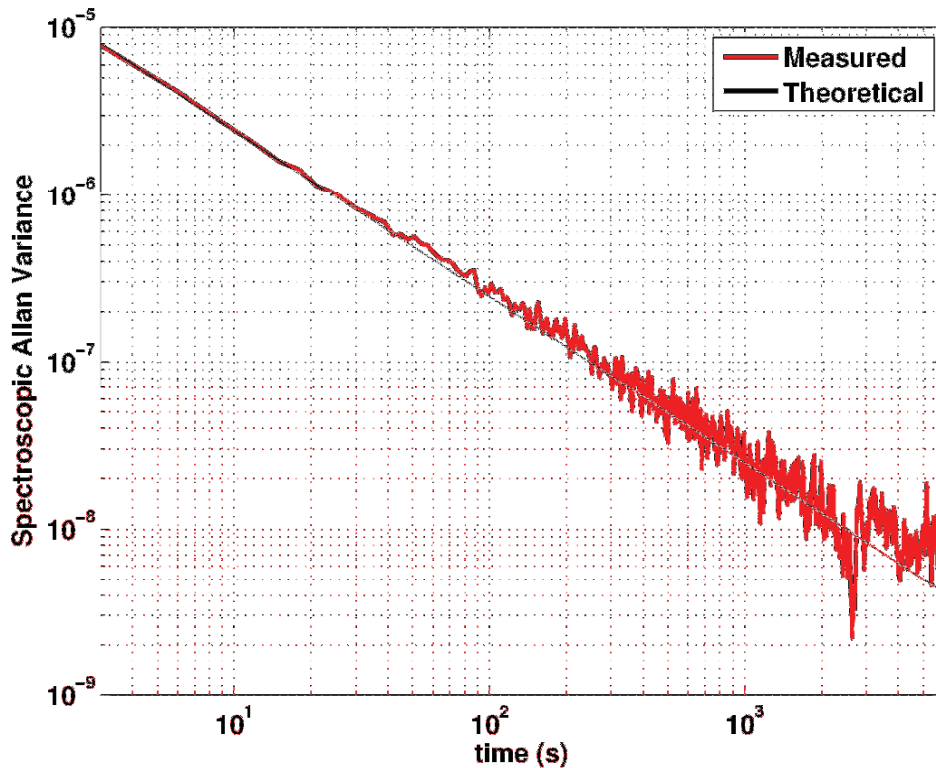


Figure 9 Plot of the Spectroscopic Allan Variance for the 750 MHz bandwidth prototype PFB. This was calculated by differencing channels 2000 and 2500. Because the entire band passes through the same analog electronics, system gain variations track extremely well across the band.

Figure 9 shows a spectroscopic Allan Variance measurement taken with the prototype PFB. A temperature-stabilized noise source was used as the input signal for this test. The Allan Variance measurements are currently limited by the stability of the signal source, not by the spectrometer, and we will be improving the stability of the signal source for future measurements of this kind. These preliminary data indicate an adequately long spectroscopic Allan Variance minimum time (4000 s) to ensure that the digital spectrometer imposes no stability constraints as far as the interval between radiometric calibrations is concerned. The total power Allan Variance was measured to be 100 s (Figure 10) which is satisfactory, but worse than expected. We have also verified that measured rms noise level is within 6% of that calculated with the radiometer equation ($\Delta T = T_{sys}/\sqrt{\beta\tau}$) assuming a noise bandwidth of 183 kHz. Half of this deviation is due to the noise bandwidth not exactly matching the filter spacing. The source of the remaining deviation and the less than perfect gain stability is under investigation. A likely candidate is low frequency pick up from power supplies.

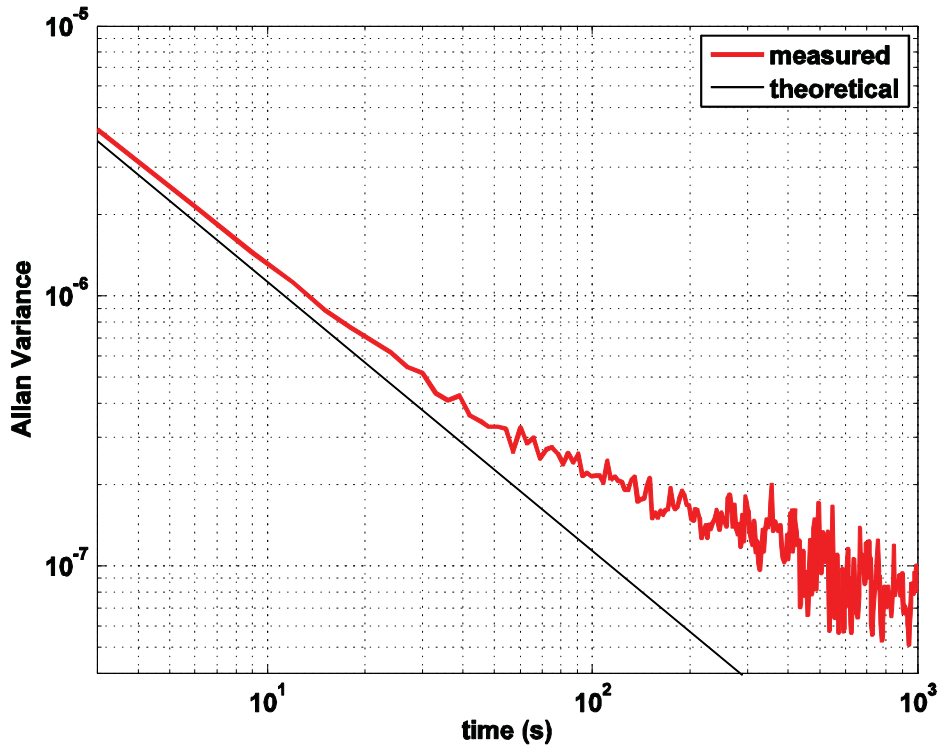


Figure 10 Plot of Total power Allan Variance for the 750 MHz bandwidth prototype PFB. The theoretical line assumes no gain drift. It also assumes a noise bandwidth equal to the channel spacing, contributing to most of the offset between the two curves at the upper left.

DYNAMIC RANGE

The ability of the spectrometer to integrate down the noise on scientific data was measured using a noise source and a frequency synthesizer modulated to produce a narrow noise-like feature (see Figure 5). The broadband noise source provides a reasonably stable signal corresponding to the front-end receiver and atmospheric noise components. The narrow bandwidth noise signal is used to simulate spectral line emission, its output periodically enabled/disabled by the controller (PC) so that successive data blocks represent signal and reference data. Figure 11 shows the input spectrum with reference signal at 130 dB and the simulated atmospheric spectral feature at 400 MHz with a power level of 97 dB (33 dB below the reference level). Note that for this particular test the rms level of the narrow signal used to represent the atmospheric signal was less than 1 bit width of the 8-bit ADC at the spectrometer frontend. This is the reason why we use the stronger noise at 750 MHz to exercise some bits of the ADC for an accurate measurement of the simulated spectral feature. The ‘atmospheric’ test signal is recovered by differencing successive signal and reference data blocks, and combining these difference signals to improve signal-to-noise. The switching time between the reference signal with the spectral feature and with no spectral feature is 60 s. The results of such a test are shown in Figure 12, which represents a total measurement time (signal plus reference) of 9252 s.

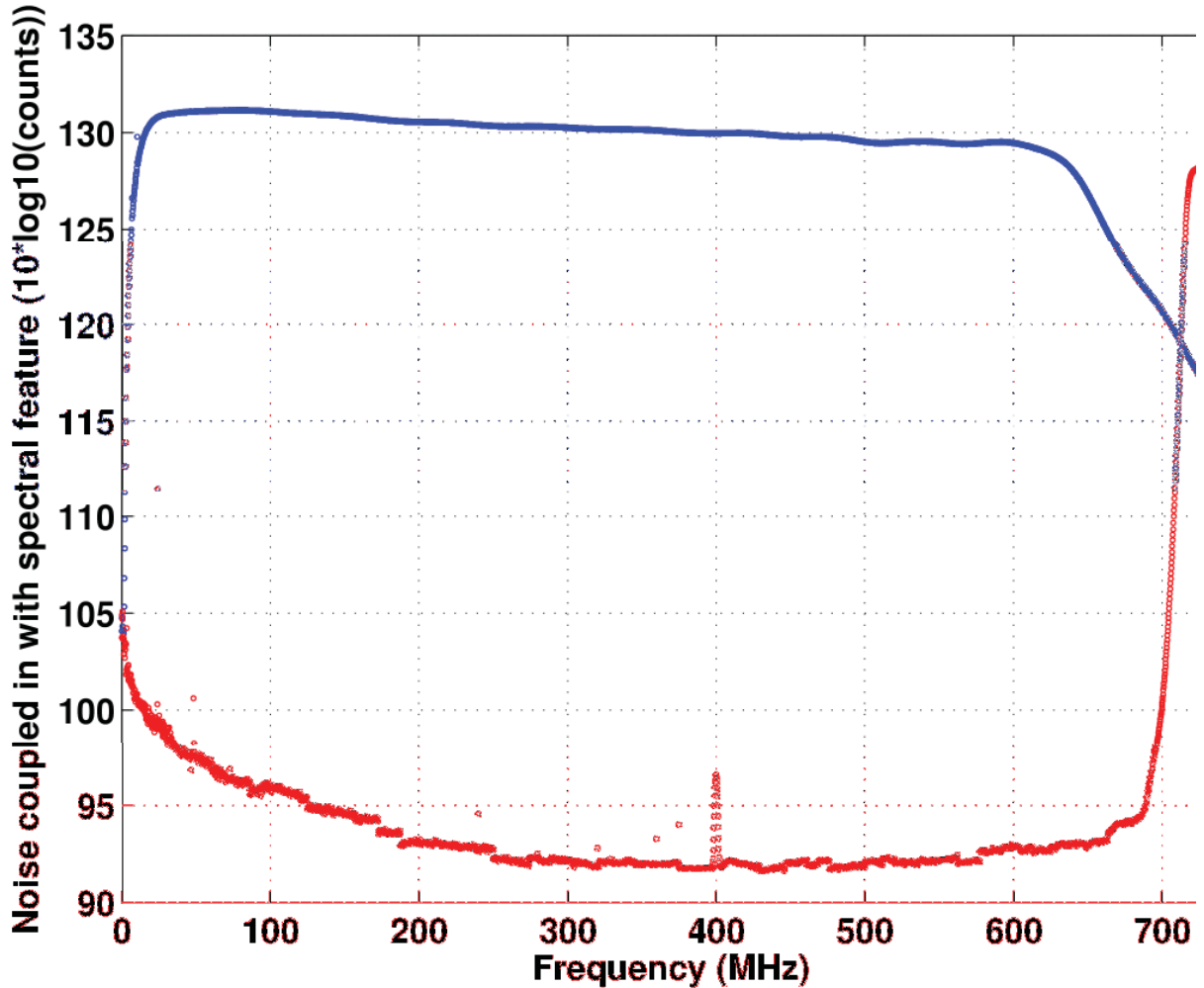


Figure 11 Spectra of simulated receiver noise coupled in with an atmospheric signal (1600 times smaller than the noise signal). See text for additional details.

These results indicate that the spectrometer has sufficient dynamic range to measure any credible atmospheric feature likely to be targeted by the proposed instruments. Related measurements on other FPGA-based PFB spectrometers have yielded similar results [1], showing signal-to-noise increasing without deviation from the ideal square root dependence for measurement times of several days.

The curve in Figure 12 shows the spectrum of the simulated receiver noise. The simulated small atmospheric spectral feature coupled in with the simulated receiver noise signature centered at 400 MHz with a bandwidth of 2 MHz. The small signal is almost 33 dB below the receiver noise level in order to simulate a 2.5 K feature being measured by a system with T_{sys} of 4000 K.

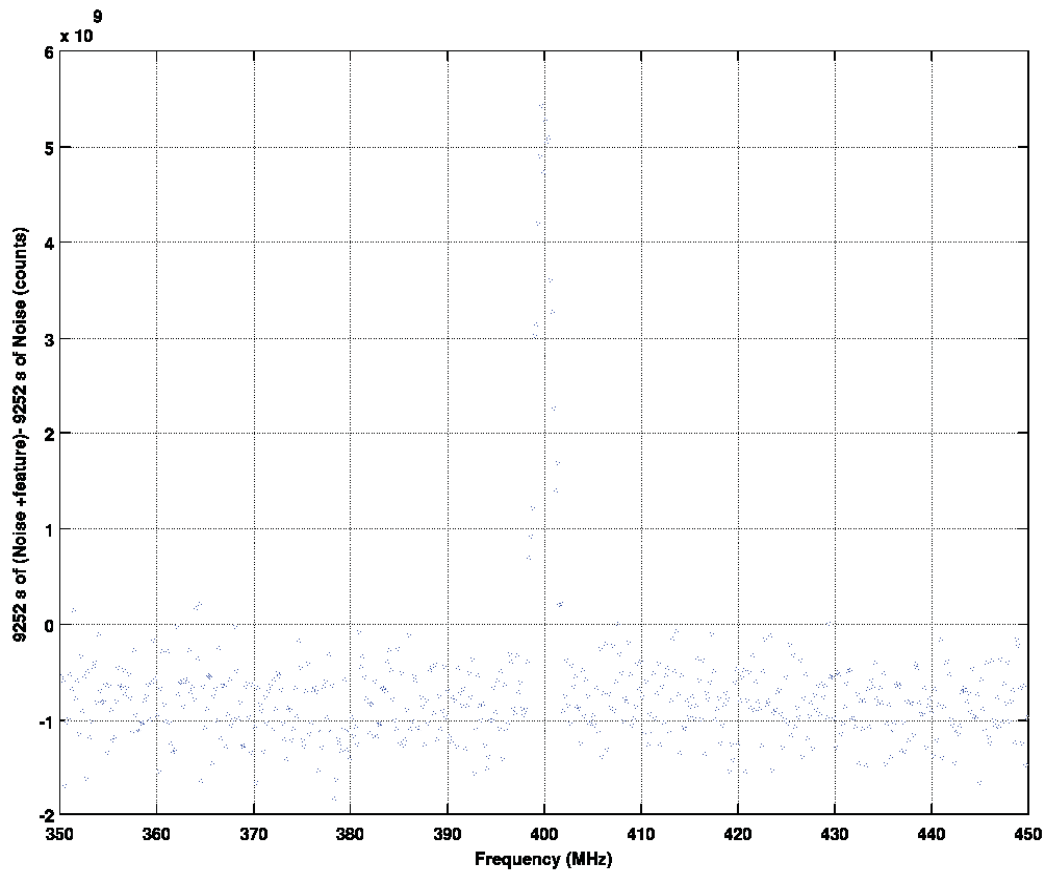
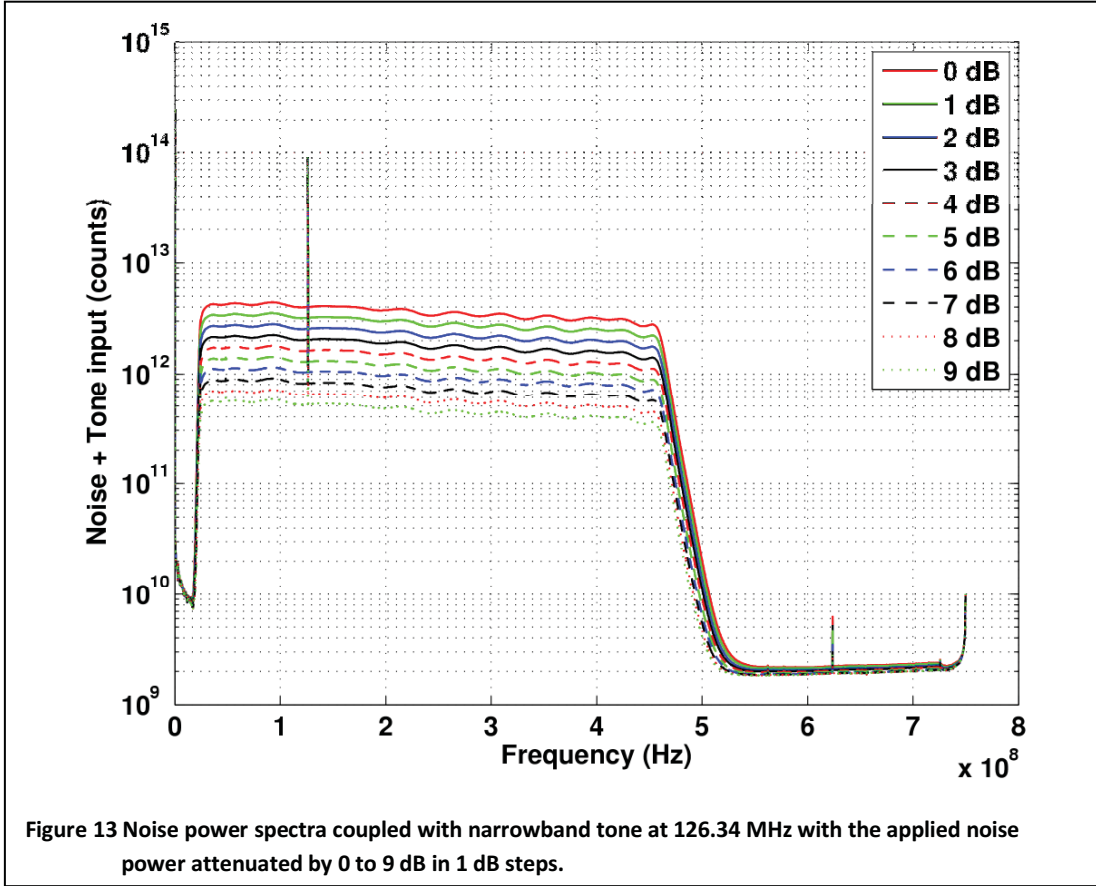


Figure 12 Output from ASIC spectrometer corresponding to the normalized difference between 9252 s of integration time on signal and the same amount of time on reference. The reference signal is the wideband noise plotted in Figure 12, and the reference is the same signal with the addition of a small filtered noise signal centered at 400 MHz.

LINEARITY

Linearity in the frequency domain is not an issue for digital spectrometers, since channel responses are determined by the sample rate of the system, and by the digital algorithms which convert the time-series data from the ADC into the frequency domain science data. Amplitude linearity is a different matter, and is one for which the entire signal chain needs to be taken into consideration. A significant consideration for the PFB is that the input signal is digitized. This action converts the continuous (analog) input signal into one which is sampled in the time domain and discrete (quantized) in the amplitude domain. In the amplitude domain it is important to realize that the input signals are relatively coarsely sampled. For the noise (Gaussian) signals representative of atmospheric emission signatures, it is important to prevent the ADC from saturating if spectral distortion is to be avoided. For the 8 bit ADC used in this spectrometer an optimal input signal level is on the order of 200 counts pk-pk, or an rms count level of ~ 35 . For signal levels below ~ 25 counts pk-pk, the response of any digital spectrometer is noticeably non-linear to both noise and tone inputs [14].



Measuring linearity at the fraction of a percent level is non-trivial. The procedure used here does not depend on an absolute calibration of the noise source. A broad band noise source with appropriate anti-aliasing filters and a variable attenuator is fed into the spectrometer. A tone that carries much less power than the noise signal is coupled into the same line and is switched on and off. For a perfectly linear system, the amplitude of this modulation will remain constant as the noise power is varied. Figure 13 shows the measured spectra as the power is scanned over 9 dB and Figure 14 shows the measured power of the tone as a function of noise power. Over a 9 dB range of input power, the measured tone varies by 2 percent. This is a direct measurement of the spectrometer gain dependence on input power. To calculate the error in the measured temperature from this small nonlinearity for a prospective instrument, the calibration procedure must be considered. A typical Schottky diode mixer receiver front end in the 500 to 600 GHz range will likely have a noise temperature of 4000 K. The calibration views will typically be cold space and an ambient target. The calibration points are thus at a system temperature of 4000 K and 4300 K respectively. For the data in Figure 14, this translates to the range from 2 to 2.15×10^{12} . The deviation from constant gain is a linear function of input power so we can write:

$$G = G_0(1 + \sigma * T) \text{ and } S = S_0 + G * T = S_0 + G_0(1 + \sigma * T)T$$

$$S_H = S_0 + G_0(1 + \sigma * T_H)T_H$$

Where T = the scene temperature, T_H = the temperature of the hot calibration, G = the gain, G_0 = the gain at $T = 0$; σ = the slope of the gain vs temperature; S = the measured signal; S_0 = the signal with a scene

temperature of 0 K (system temperature of 4000 K) and S_H = the signal with a scene temperature for the ambient target assumed to be 300 K (system temperature of 4300 K).

$$\sigma = -2.33 * 10^{-6} \text{K}^{-1}$$

The standard calibration scheme is to linearly interpolate between the hot and cold calibration values giving:

$$T' = \frac{S - S_0}{S_H - S_0} * T_H$$

where T' = the interpolated value for T .

Substituting the equation for S and S_H gives

$$T' = \frac{S_0 + G_0(1 + \sigma * T)T - S_0}{G_0(1 + \sigma * T_H) * T_H} * T_H$$

$$T' = \frac{(1 + \sigma * T)T}{(1 + \sigma * T_H)} \cong (1 + \sigma * T)(1 - \sigma * T_H)T \cong T - \sigma(T_H - T)T$$

The error in T' then is $T - T' \cong \sigma(T_H - T)T$ The maximum error occurs for $T = 150\text{K}$ where

$$T - T' \approx 0.05\text{K}$$

This is more than adequate for currently planned missions. This calculation is appropriate for a spectrally flat scene. For a scene with spectral content the biggest error occurs for a narrow spectral feature on a cold background. Here the gain = G_0 , but the calculated gain = $G_0(1 + \sigma * T_H)$. This leads to a 0.07% over estimation of the strength of a narrow spectral line.

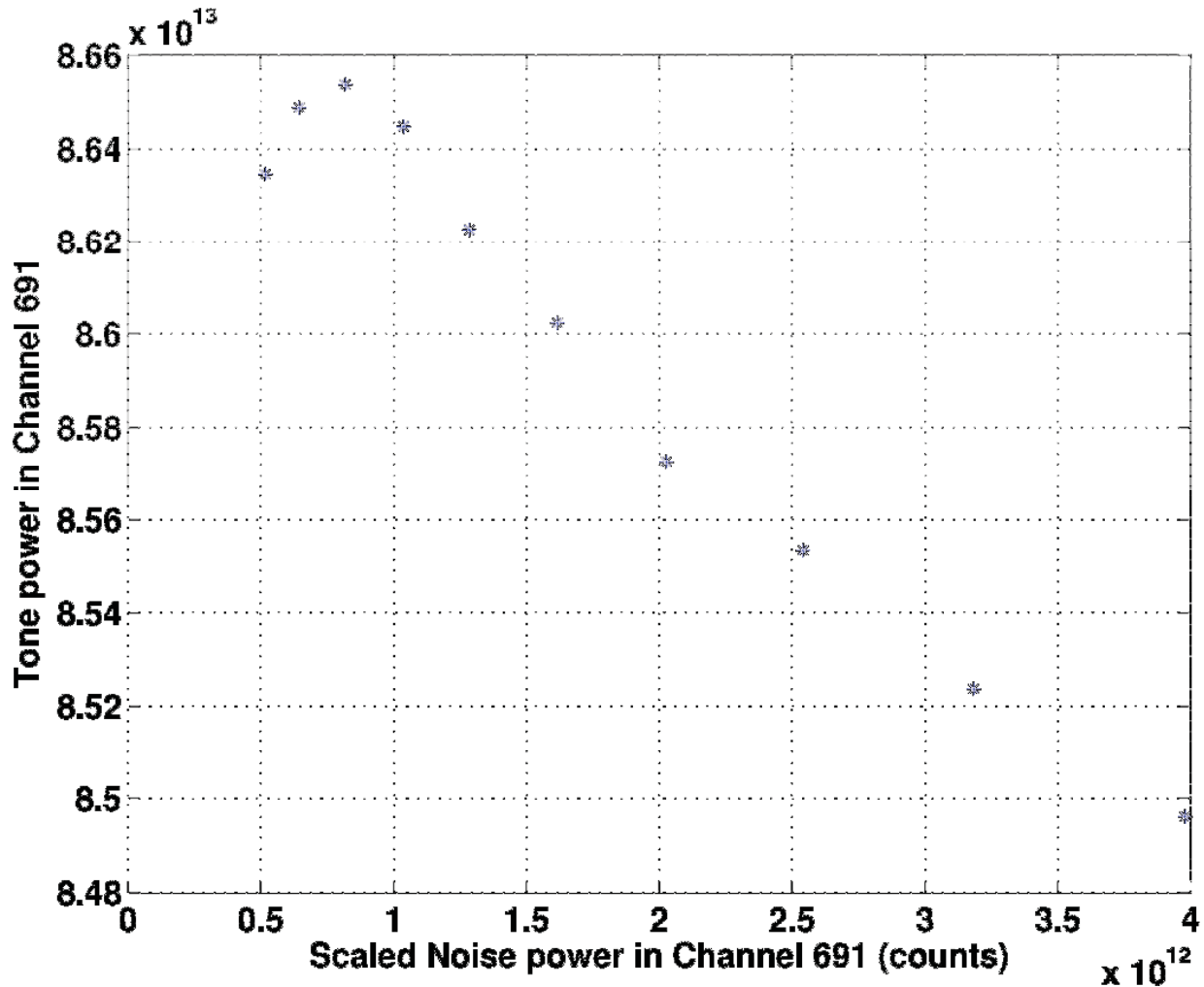


Figure 14. Dependence of the measured tone power (at 126.34 MHz) on the applied noise power, with the noise power varying by almost an order of magnitude.

RADIATION TESTING

As part of the ASIC chip evaluation, the Berkeley team performed some important radiation testing. Even though it was not fabricated in a radiation-hard process, the ASIC was designed to have adequate total dose radiation hardness to support missions throughout the inner solar system. The 90 nm ST process used to fabricate this chip is similar to the 90 nm TSMC one used to fabricate the digital autocorrelators on Aura MLS. These autocorrelators have operated continuously for over 5 years in orbit with no issues. Some design rules were modified (compared to standard designs implemented in this ST process), particularly in the I/O buffers, to reduce susceptibility to latch-up. In addition, the logic, memory and control registers within the ASIC were implemented in a way that an SEU which changed the state of a bit would only impact the data in a single output spectrum – i.e., no persistent error would

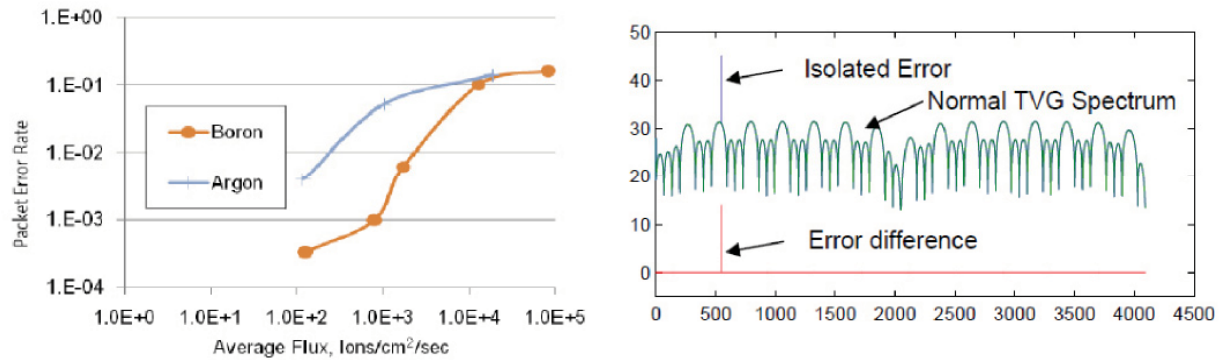


Figure 15 Radiation test results on the ASIC chip. The left panel shows the data corruption rate versus flux for two types of heavy ion (10 MeV), with spectra accumulated every 21 ms. The right hand panel shows an example of a corrupted spectrum (plotted with the vertical axis on a \log_2 scale). These demonstrate that SEUs can be identified readily in the data stream, in general they do not cause erratic behavior, and the expected rate of SEUs is low.

remain as the result of an SEU. This was validated using the built-in test vector generator (TVG) during radiation testing.

An important design-for-test (DFT) feature of the ASIC is the inclusion of several multiple-input shift registers (MISRs) which allow intermediate points in the data flow within the chip to be externally monitored or forced. These registers were used to determine where the single event upsets were arising during radiation testing, and some key results are shown in Figure 15. The chip was designed to not latch-up and no latch-ups were observed during the radiation tests.

SUMMARY

The digital polyphase spectrometer provides the desired bandwidth and resolution to meet the science needs of an Inner Solar System flight instrument. The previously flown CTS provided insufficient bandwidth, and consumed significantly higher resources (mass, volume and power) than the digital spectrometer. The digital implementation of the polyphase spectrometer provides excellent repeatability and long-term stability, reducing calibration and environmental requirements. Other digital spectrometers such as the autocorrelator and FFT implementations share many of the advantages of the polyphase design, but provide inferior channel shapes and/or poorer signal-to-noise.

ACKNOWLEDGEMENT

The work described in this report was carried out at the Jet Propulsion Laboratory, California Institute of Technology under a contract with the National Aeronautics and Space Administration

The authors acknowledge students, faculty and sponsors of the Berkeley Wireless Research Center, chip fabrication donation of STMicroelectronics, NSF Infrastructure Grant No. 0403427, C2S2

BIBLIOGRAPHY

[1] Venus Flagship Mission Study. <http://vfm.jpl.nasa.gov/>

[2] Zurek, R. W., A. Chicarro, M. A. Allen, JL Bertaux, R. T. Clancy, F. Daerden, V. Formisano, J. B. Garvin, G. Neukum, M. A. Smith, 2009: Final Report from the 2016 Mars Orbiter Bus Joint Instrument Definition Team (JIDT), November 2009.

- [3] The Europa Jupiter System Mission, April 2009.
<http://opfm.jpl.nasa.gov/europajupitersystemmission/ejsmpresentations/>
- [4] Titan Explorer Public Report, January 2008. <http://www.lpi.usra.edu/opag/>
- [5] Personal Communication with Dr. Mark Allen at JPL.
- [6] Richards, B. et al., A 1.5GS/s 4096-Point Digital Spectrum Analyzer for Space-Borne Applications IEEE Custom Integrated Circuits Conference, September 2009
- [7] Jarnot R., Perun V. and Schwartz M., "Radiometric and Spectral Performance and Calibration of the GHz Bands of EOS MLS", *IEEE Trans. Geosci. and Remote Sensing*, vol. 44, no. 5, pp. 1131-1143, May 2006.
- [8] Acousto-Optical Spectrometers in Space, Schieder, R., Horn, J., Siebertz, O., Klumb, M., Frerick, J., & Tolls, V, Submillimetre and Far-Infrared Space Instrumentation, Proceedings of the 30th ESLAB Symposium held in Noordwijk, 24-26 September 1996. Edited by E.J. Rolfe and G. Pilbratt. ESA SP-388. Paris: European Space Agency, 1996., p.187
- [9] Hartogh P. and Osterschek K., "Multiband chirp transform for microwave remote sensing of middle-atmospheric trace gases", *Proc. SPIE*, vol. 2583, 282, 1995.
- [10] Gulkis, S., Frerking, M., Crovisier, J., et al., MIRO: Microwave Instrument for Rosetta Orbiter, *Sp. Sci. Rev.*, 2007, vol. 128, pp. 561–597.
- [11] Lucas Paganini, "Power spectral density accuracy in chirp transform spectrometer" Ph.D. dissertation, Max Planck Institute of Solar System Research, Germany, 2008.
- [12] Werne, T. A., Jarnot, R.F., Allen, M. A., FPGA-Based Hardware/Software Co-Design Instrument Command-and-Control Solutions, JPL Technical Report D10-1559. <http://hdl.handle.net/2014/41552>
- [13] A 256 MHz Bandwidth Baseband Receiver/Spectrometer, Ferris R.H., and S.J. Saunders, *Experimental Astronomy* (2004) 17:(269-277).
- [14] Quantization with 4 bits, <http://casper.berkeley.edu/memos/p011.quant.pdf>
- [15] Harris, F.J, Dick, C., Rice, M., "Digital Receivers and Transmitters Using Polyphase Filter Banks for Wireless Communications", *IEEE TRANSACTIONS ON MICROWAVE THEORY AND TECHNIQUES*, VOL. 51, NO. 4, APRIL 2003